EFFICIENT EMBEDDING-GENERATION SERVING WITH HETEROGENEOUS BATCHING

Anonymous authors
Paper under double-blind review

ABSTRACT

Modern information retrieval increasingly relies on both embedding and generative models to achieve high accuracy. To make such applications more responsive, the underlying serving systems must be optimized for mixed workloads. Yet, current systems suffer from low throughput and poor GPU utilization, primarily because they cannot batch embedding and generation requests together. We address this bottleneck with heterogeneous batching, which schedules embedding and generation requests within the same batch. Realizing this idea requires two changes to the system internals: a *unified kernel abstraction* and *fine-grained intra-batch scheduling*. The unified abstraction enables concurrent handling of embedding and generation, while the intra-batch scheduler dynamically adapts batch composition to balance end-to-end throughput across both tasks. Our evaluation with four A100 GPUs shows that heterogeneous batching achieves 1.28×-4.52× higher throughput and 35.8-52.0% lower latency than default vLLM.

1 INTRODUCTION

Modern information retrieval (Asai et al., 2023; Gao et al., 2023; Jiang et al., 2023b; Shao et al., 2023) employs both embedding and generative models for improved accuracy. A query is first *embedded* for dense retrieval, and then a subsequent query is *generated* capturing missing information. This iteration continues until sufficient information is retrieved. Accordingly, search becomes more responsive when the model serving is efficient for mixed embedding and generation workloads.

Yet, existing systems provide low throughput and poor GPU utilization for mixed workloads. Serving systems (e.g., Kwon et al. (2023)) run each model separately. With multiple GPUs, some deployments can handle embeddings and others generation, but this causes two problems: (i) predicting the right embedding-generation ratio is hard, and (ii) changing the split requires costly model reloading. Even with perfect knowledge of future workloads, GPU-level split delivers suboptimal performance as embedding servers are compute-bound and generation servers are memory-bound. We hypothesize that homogeneous batching is a fundamental bottleneck in leveraging GPU resources efficiently.

In this work, we present a systems approach for efficiently serving mixed embedding-generative workloads. Our key idea is to unify the two distinct compute patterns—embedding and generation—into a single abstraction, enabling heterogeneous batching within a single inference step. Embedding and generation kernels both inherit this abstraction and access their respective parameters. This design allows fine-grained load balancing and improved GPU utilization, yielding substantially higher throughput. It requires no additional training and applies broadly to existing models.

Designing our system involves two high-level considerations: (i) unified abstraction and (ii) heterogeneous batching. We pursue high throughput and optimal intra-batch scheduling as follows:

- ***Unified abstraction***: Our abstraction κ takes the current state and tokens (ϕ_{t-1}, τ_t) to produce a new state ϕ_t, where ϕ_t represents data retained in GPU global memory. This abstraction implies that tokens are processed in a streaming fashion. Nearly all existing embedding kernels violate this pattern. Our new embedding kernel adheres to it with *incremental pooling*.[1]

[1]We have noticed that the latest version of vLLM, developed concurrently, introduced a similar incremental strategy to handle long context.

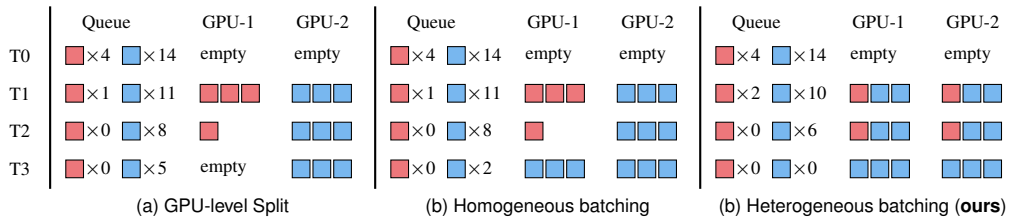

Figure 1: Example embedding-generation workload processing. Workload is given at T0. Both (a) GPU-level split and (b) homogeneous batching on a combined model cannot complete all requests by T3. Our proposed heterogeneous batching completes all 18 units of workloads (4 + 14).

- ***Optimal batching***: Our heterogeneous batching aims to balance the end-to-end throughput between embedding and generation under dynamic workloads. Our system achieves higher throughput when compared to every possible GPU-level split.

Fig. 1 demonstrates a mixed workload for which heterogeneous batching can be more efficient than other options. A mixed workload is submitted at time 0 (T0), where the number of red and blue boxes in the Queue indicates the amount of remaining workload. GPU-level split, with some GPUs dedicated to embedding and others to generation, cannot utilize GPU resources if the workload doesn't perfectly match a pre-determined split. Likewise, homogeneous batching cannot fully utilize available GPU memory (at T2). Our proposed heterogeneous batching completes the workload by fully utilizing GPUs' compute and memory resources. We analyze this formally in Section 3.

Our technique is practical and delivers high performance. We implemented our prototype system (called ORTHRUS) on top of vLLM version 0.92, without modifying memory management or model specification. Evaluation on four NVIDIA A100 GPUs with state-of-the-art open-weight models shows ORTHRUS delivers 1.28×-4.52× higher normalized throughput[2] than GPU-level splits, without any approximation on the inference results, for mixed embedding and generation workloads.

This work is orthogonal to memory-efficient model composition. Specifically, embedding and generative models can share a large fraction of parameters through LoRA adapters (Vasani et al., 2025; Gauthier, 2024) or by training a combined model (Muennighoff, 2022; Zhang et al., 2025; Springer et al., 2024; Li et al., 2024). While this work benefits from these advances, we advance compute patterns inside GPU kernels. This work is also orthogonal to efficiently scheduling multiple LoRA adapters (Sheng et al., 2024a; Chen et al., 2024); we focus on designing an effective kernel for heterogeneous batching rather than combining existing ones.

In summary, this work makes the following technical contributions:

1. To our knowledge, we are the first to propose, design, and implement heterogeneous batching of embedding and generation requests within each inference step.
2. We formalize our approach with a unified runner abstraction and throughput-aware intra-batch scheduling. We have open-sourced our system including evaluation scripts and data.[3]
3. We evaluate our system (ORTHRUS) from multiple angles to demonstrate higher throughput, reduced latency, instant load balancing, low overhead, and generalization to existing models.

The rest of this paper is organized as follows. Section 2 discusses our technical novelty in relation to existing literature, Section 3 presents our system, and Section 4 evaluates our system. Finally, Section 5 summarizes this work.

2 RELATED WORK

2.1 EMBEDDING AND GENERATION FOR MODERN INFORMATION RETRIEVAL

Knowledge-intensive tasks increasingly combine embedding and generative models in iterative pipelines that refine retrieval and improve answer quality. Embedding models capture dense semantic similarity for document retrieval, while generative models synthesize or reformulate queries

[2] *Normalized throughput* rescales throughput so embedding and generation are comparable (see Section 4.1).
[3] Our system is open-sourced at `https://anonymous.4open.science/r/Orthrus-483B`.

and answers (Gao et al., 2023; Wang et al., 2023; Shen et al., 2024). Retrieval-Augmented Generation (RAG) (Lewis et al., 2020) grounds generation in retrieved evidence, and recent work extends this paradigm with iterative retrieval and reasoning (Asai et al., 2023; Jiang et al., 2023b; Shao et al., 2023; Trivedi et al., 2023; Lyu et al., 2024). These methods highlight the effectiveness of embedding–generation loops, but also demand efficient inference for mixed workloads. Our system addresses this challenge by improving inference efficiency and responsiveness for such pipelines.

2.2 Efficient parameter sharing between embedding and generative models

State-of-the-art embedding models are increasingly derived from generative models via parameter-efficient fine-tuning, most commonly with LoRA. Models such as GTE-Qwen2-7B-instruct (Li et al., 2023), E5-Mistral-7B (Wang et al., 2024), SFR-Embedding-Mistral (Meng et al., 2024), RepLLaMA-7B-Passage (Ma et al., 2024), and LLM2Vec (BehnamGhader et al., 2024) fine-tune base models like Qwen2, Mistral, or LLaMA, reusing nearly all parameters while adding lightweight adapters. This trend shows that embedding and generative models share substantial weights, with task-specific behavior introduced through adapters.

Beyond fine-tuning, several works train models to support both capabilities directly. Adapting generative transformers (Muennighoff et al., 2024), using transformers without modification (Muennighoff, 2022), or introducing summary tokens as embeddings (Zhang et al., 2025). Other methods derive embeddings from repeated inputs (Springer et al., 2024) or jointly optimize retrieval and generation with aligned representations (Li et al., 2024; Tang et al., 2025).

Together, these approaches demonstrate the feasibility of parameter sharing across embedding and generation tasks, but they focus on model training and design. The equally important challenge of efficiently serving such unified models at inference remains largely unexplored. Our work addresses this gap by enabling efficient serving of embedding and generation workloads under mixed demands.

2.3 Lack of heterogeneous batching in serving systems

Existing serving systems are optimized for generative workloads, structuring scheduling and batching around the autoregressive decode loop. A common baseline is to process requests in First-Come-First-Serve (FCFS) order or enforce client rate limits, which simplifies batching but ignores workload diversity. More advanced systems improve on this baseline in different ways: Orca (Yu et al., 2022) introduced *iteration-level scheduling*, running one decode step per iteration so requests can enter or leave dynamically. vLLM (Kwon et al., 2023) added *PagedAttention* for efficient KV-cache management. Sarathi-Serve (Agrawal et al., 2024) proposed *chunked prefill* to reduce stalls from large prompts. Other directions include *kernel fusion* (Wang et al., 2021; Fang et al., 2021), *memory offloading* (Sheng et al., 2023), *prefill/decode disaggregation* (Patel et al., 2024; Zhong et al., 2024; Hu et al., 2024), *preemptive scheduling* (Wu et al., 2024), and *fair scheduling* (Sheng et al., 2024b). Despite these advances, all assume decode-oriented workloads. Embedding requests, which involve only prefills, either wait behind long decodes or fragment batches when mixed naively.

Another line of work addresses multi-tenant serving by co-locating LoRA adapters. SLoRA (Sheng et al., 2024a) unified paging for adapter weights, and Punica (Chen et al., 2024) develops segmented gather kernels for batching LoRA variants. These systems improve throughput when serving many LoRA adapters, but still assume generation-only workloads. Crucially, embedding and generation require different *processing steps*. Generation performs sampling, whereas embedding pool hidden states into a fixed-length vector. Prior systems treat every request as a decode loop, forcing embeddings to be deployed as a separate service. Our system instead enables *heterogeneous batching*, efficiently co-serving embedding and generation workloads on the same infrastructure.

3 Unified Model Runner for Heterogeneous Batching

To utilize GPU resources more efficiently, we propose heterogeneous batching of embedding and generation requests. First, we describe our design for heterogeneous batching. Second, we introduce a mathematical model to show that heterogeneous batching can achieve higher throughput. Finally, we continue our formal analysis to study how we should compose each batch for low latency.

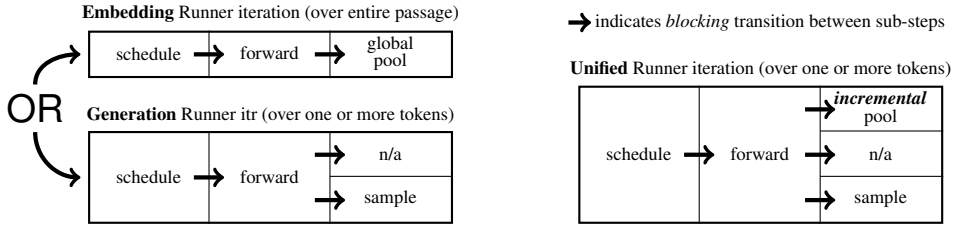

(a) Exclusive iterations for embedding/generation (b) Unified iteration for heterogeneous batching

Figure 2: Runner structure comparison. The conventional approach presented on the left is designed for completely separate embedding and generation serving. Combining them is challenging due to the discrepancy between global aggregation vs token-level sampling. Our unified runner performs incremental pooling, allowing efficient concurrent processing of embedding and generation requests.

3.1 Unified Runner for heterogeneous batching

At a very high level, our runner is designed for iteration-level batching (Yu et al., 2022), aiming for seamless integration with the vLLM (Kwon et al., 2023)'s open-sourced model management and asynchronous server. Yet, our approach differs from existing approaches in that both embedding and generation requests are processed using the same runner, which we achieve by consolidating distinct embedding and generation runners into one in a structured way.

Our runner operates in three blocking stages: (1) `schedule`, (2) `forward`, and (3) `emit` (see Fig. 2 for illustration). `Schedule` determines batch composition, including generation prefills, decodes, or embedding chunks. `Forward` applies attention and feed-forward layers, identical across request types except for input length. `Emit` diverges: generation samples the next token, while embedding performs *incremental pooling* to maintain statistics for the final representation $\mathcal{P}(H)$. Because prefills are *chunked*, hidden states $H = \{H_t\}_{t=1}^{n}$ arrive incrementally; the aggregator avoids materializing all H_t by keeping only minimal state. A running sum S and count n for mean pooling, the most recent H_t for last-token pooling, or the full sequence if required. This ensures consistency under chunked execution while enabling concurrent embedding and generation.

Implementation The vLLM architecture consists of four components: an asynchronous server, a scheduler, model runners, and a memory manager based on PagedAttention. Our modifications focus on the scheduler and model runner. We introduce a *unified model runner* that combines the generative and pooling runners, executes the forward pass, and invokes sampler and pooler kernels in parallel. We also add a scheduling policy that constructs heterogeneous batches while remaining compatible with vLLM's execution model. On the kernel side, we implement Triton-based incremental pooling operators that run concurrently with sampling, and an embedding prefill kernel built on FlashAttention. Recent versions of vLLM support chunked prefill for embeddings with mean pooling to handle long prompts. Our design generalizes this to arbitrary pooling operators and integrates them into heterogeneous batching, allowing embeddings and generations to be processed concurrently. For embeddings, LoRA weights are pinned in GPU memory, with request indices passed to selectively apply low-rank updates.

3.2 Throughput analysis: homogeneous vs heterogeneous batching

We formally analyze the throughput difference between homogeneous and heterogeneous batching. This analysis indicates heterogeneous batching can achieve higher efficiency because embedding requests can be *squeezed* into the same batch containing generation requests. Unlike prior analytical models of LLM serving that focus on prefill/decode scheduling under FCFS assumptions (Yu et al., 2022; Agrawal et al., 2024), our formulation explicitly incorporates both embedding and generation workloads into the same iteration-based batch model.

A workload consists of w_e embedding and w_g generation requests. An embedding request takes s_e steps to complete, and a generation request takes s_g steps. We have M memory; scheduling an embedding request consumes m_e memory, and a generation request consumes m_g memory. Let

$s_g = F \cdot s_e$, $m_g = F \cdot m_e$ and $M = L \cdot m_e$, where $F \geq 1$ captures the general phenomenon that generation requires more steps (for decoding) and memory (for KV cache).

Let $L = kF + r$ with $0 < r < F$ for some $k = \lfloor L/F \rfloor$. The number of steps T_{homo} required by homogeneous batching for completing the workload is:

$$T_{homo} = \left\lceil \frac{w_e}{L} \right\rceil + \left\lceil \frac{Fw_g}{\lfloor L/F \rfloor} \right\rceil = \left\lceil \frac{w_e}{L} \right\rceil + \left\lceil \frac{F^2 w_g}{L - r} \right\rceil$$

Heterogeneous batching can leverage memory more effectively by filling in r *slots* with embedding requests, as follows:

$$T_{hetro} = \left\lceil \frac{w_e + F^2 w_g}{L} \right\rceil$$

Heterogeneous batching can thus reduce the total number of steps as follows:

$$T_{homo} - T_{hetro} \approx \underbrace{\left(\left\lceil \frac{w_e}{L} \right\rceil + \left\lceil \frac{F^2 w_g}{L} \right\rceil - \left\lceil \frac{w_e + F^2 w_g}{L} \right\rceil \right)}_{\in [0,1]} + \underbrace{\left(\left\lceil \frac{F^2 w_g}{L - r} \right\rceil - \left\lceil \frac{F^2 w_g}{L} \right\rceil \right)}_{\text{extra penalty from } r \geq 0}$$

Heterogeneous batching is almost always more efficient than homogeneous batching, and the gap widens when generative requests produce long answers that require more memory, resulting in a larger r. This analysis is based on an assumption that is actually favorable to homogeneous batching: it presumes that adjusting the GPU split ratio incurs zero overhead and that context switching between embedding and generation is instantaneous. In practice, neither of these assumptions holds, which further increases the performance gap between homogeneous and heterogeneous batching.

3.3 Intra-batch Scheduling (IBS) for low-latency serving

With heterogeneous batching, any scheduling policy can deliver near-identical throughput; however, their latencies may differ. In this section, we analyze the optimal batch composition for minimizing the request-level latency. We aim to ensure "first come, first served" within each embedding/generation queue; however, some later generations may be scheduled before earlier embeddings (or vice versa) to reduce latency.

We have w_e embedding and w_g generation requests at time 0. Let (x, y) be the number of embedding and generation requests scheduled within a batch. $x + Fy \leq L$. Set $t_e = 1$ without loss of generality.

- **Embeddings.** x requests complete in each step (since $t_e = 1$). j-th embedding (in the queue) completes at j/x. The average embedding latency is then:

$$\bar{T}_e(y) \approx \frac{w_e}{2x} = \frac{w_e}{2(L - Fy)}$$

- **Generation.** We finish y requests every F steps (since $t_g = F \cdot t_e = F$). The k-th *group* of size y thus completes at kF. The average generation latency is:

$$\bar{T}_g(y) \approx \frac{Fw_g}{2y}$$

The average latency across embedding and generation requests $\bar{T}(y)$ is a weighted mean of $\bar{T}_e(y)$ and $\bar{T}_g(y)$, expressed as:

$$\bar{T}(y) = \frac{w_e \bar{T}_e(y) + w_g \bar{T}_g(y)}{w_e + w_g} \quad \propto \quad f(y) = \frac{w_e^2}{L - Fy} + \frac{Fw_g^2}{y} \quad \rightarrow \quad y^* = \frac{Lw_g}{w_e + Fw_g}$$

where y^* is obtained by setting $f'(y) = 0$. Finally, we get $x^* : y^* = w_e : w_g$, indicating the batch composition should be dynamically adjusted to match the respective queue size.

4 Evaluation

We evaluate Orthrus, an embedding-generation serving system with heterogeneous batching. The setup is described in Section 4.1. Our results show that:

- ***Throughput:*** ORTHRUS improves average throughput under mixed embedding and generation workloads by 1.28×-4.52×, compared to GPU-level model splits (Section 4.2).
- ***Low Latency with Intra-batch Scheduling (IBS):*** IBS improves request-level latency. ORTHRUS improves p99 generation latency by 9% compared to GPU level split baselines, and p99 embedding latency by 16% compared to naive scheduling baselines (Section 4.3).
- ***High GPU utilization:*** ORTHRUS achieves higher average GPU utilization by 40.6 percentage points, allowing it to complete a mixed workload, an average of 43% faster (Section 4.4).
- ***Minimal Overhead:*** ORTHRUS's combined batching of embedding and generation requests sustains nearly the same throughput as running on dedicated GPUs, with embedding throughput reduced only by the expected overhead of LoRA (Section 4.5).
- ***Model Generalizability:*** ORTHRUS works across different models and LoRA adapters; we validate it on 3 models with LoRA ranks up to 64, showing consistent improvements (Section 4.6).

4.1 BASELINE DEPLOYMENT SCENARIOS AND EVALUATION WORKLOADS

Baselines We compare ORTHRUS against several baselines. (***SplitGPU***) A deployment that runs separate models on separate GPUs. We denote the number of GPUs dedicated to embedding and generation as $X:Y$, written $\text{SplitGPU}_{\text{X:Y}}$. For example, $\text{SplitGPU}_{1:3}$ means one GPU serves embedding while three GPUs serve generation. (***SameGPU***) A setup where both embedding and generation requests share a single GPU but are processed sequentially without heterogeneous batching. In this case, requests alternate in a first-come, first-served manner (FCFS). (***Scheduling policies***) We consider two methods. FCFS batches requests across types without prioritization. IBS (ours) allocates slots proportionally to the number of embedding and generation requests in the queue.

Workloads and Models For ORTHRUS, embedding and generation requests are co-located on a GPU, using LoRA adapters for the embedding models. We use the Mistral 7B model (Jiang et al., 2023a) and the LoRA adapter for the e5-mistral-7b-instruct model (Wang et al., 2024) for our experiments. For SplitGPU deployments, e5-mistral-7b-instruct with the combined weights are used for embedding requests. We test with additional models in Section 4.6.

We generate synthetic workloads that simulate a mix of embedding and generation requests. Embedding requests consist of 128 tokens, while generation requests consist of a prompt of 128 tokens and a generation length of 512 tokens. We vary the ratio of embedding to generation requests to evaluate performance under different workload mixes.

Hardware We run experiments on a Slurm cluster with 4 NVIDIA A100 40GB GPUs. Each GPU runs a vLLM deployment (SplitGPU or ORTHRUS), and requests are distributed evenly across the 4 GPUs using round-robin scheduling. Clients issue requests asynchronously, so multiple requests may be in flight concurrently on each GPU.

Throughput Metric We report throughput as completed requests per second, normalizing embedding and generation requests to account for their different compute costs. Let T_{gen} and T_{embed} be the per-second request rates. Normalized throughput is $T_{\text{norm}} = 1.7 \cdot T_{\text{gen}} + T_{\text{embed}}$ where $1.7 \approx 21.9/12.9$ is the ratio of saturated embedding to generation throughput on our setup. This makes embedding and generation workloads comparable, following prior work on long decode vs. short prefill workloads (Zhong et al., 2024; Agrawal et al., 2024; Narayanan et al., 2020).

4.2 ORTHRUS IMPROVES THROUGHPUT

We evaluate the throughput of ORTHRUS across different ratios of requests, comparing against SplitGPU deployments and alternative schedulers. The experiment uses 512 clients, measured over 180 seconds after a 180-second warm-up. Fig. 3a reports normalized throughput. SplitGPU deployments underutilize GPUs when workload ratios diverge from the static split. For example, $\text{SplitGPU}_{1:3}$ and $\text{SplitGPU}_{3:1}$ both show significant drops when the workload skews away from their fixed allocation. SameGPU with FCFS improves utilization but suffers when workloads are balanced (e.g., 40–60% generation), as alternating schedules prevent full GPU usage. In contrast, ORTHRUS with FCFS and IBS achieves near-optimal throughput across all ratios. We discuss the limitations of FCFS in Section 4.3, and show how IBS avoids these issues while maintaining high throughput.

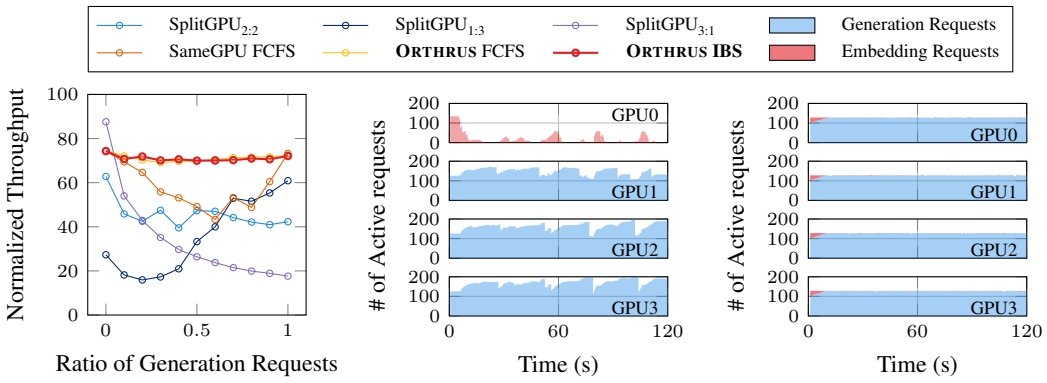

(a) Overall Throughput (b) Active Requests over time ($SplitGPU_{1:3}$) (c) Active Requests over time (ORTHRUS (IBS))

Figure 3: Throughput and GPU utilization comparison. (Fig. 3a) shows normalized throughput of existing serving techniques vs our heterogeneous batching, ORTHRUS. (Fig. 3b, Fig. 3c) shows request timelines for $SplitGPU_{1:3}$ and ORTHRUS under a 75% generation / 25% embedding workload. Each timeline reports the number of active requests per GPU. ORTHRUS fully utilizes all GPUs, while $SplitGPU_{1:3}$ leaves some underutilized.

Fig. 3b and Fig. 3c show GPU utilization under a workload of 75% generation and 25% embedding requests. In $SplitGPU_{1:3}$, the embedding GPU remains underutilized due to fixed model assignment, whereas ORTHRUS fully utilizes all GPUs with both request types. This highlights the limitation of static model placement: even when the GPU split (e.g., 1:3) matches the workload ratio, homogeneous batching leaves capacity unused due to variable decode lengths. As shown in Section 3.2, heterogeneous batching is inherently more efficient, as it can fill residual capacity in generation batches with embeddings, achieving higher throughput regardless of split accuracy. ORTHRUS adapts to workload dynamics and sustains high throughput across all ratios.

4.3 ORTHRUS WITH INTRA-BATCH SCHEDULING (IBS) REDUCES LATENCY

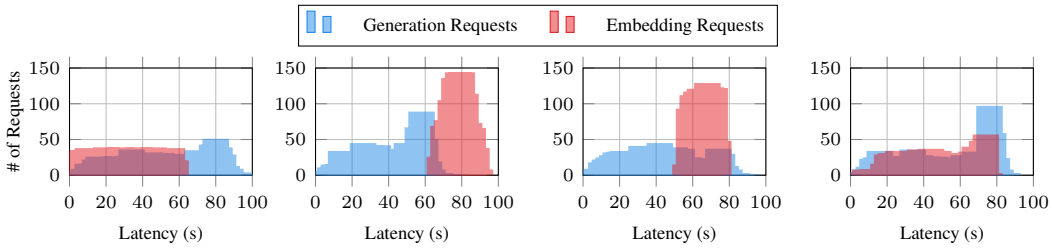

(a) $SplitGPU_{1:3}$ (b) SameGPU (FCFS) (c) ORTHRUS (FCFS) (d) ORTHRUS (IBS)

Figure 4: Latency distributions with various serving methods. Vertical bars appearing on the left side indicate lower latencies. The workload consists of 1,000 generations followed by 1,000 embeddings, all submitted at time 0. ORTHRUS with IBS achieves 9% lower p99 generation latency than SplitGPU, and up to 16% faster embedding latency than other schedulers.

We evaluate the latency distribution of embedding and generation requests under a workload where 1,000 generation requests are submitted immediately before 1,000 embedding requests. We measure per-request latency and plot the distributions in Fig. 4.

$SplitGPU_{1:3}$ allocates 3 GPUs to generation requests, and 1 GPU to embedding requests. Since requests are queued separately, embedding latency is unaffected by generation. However, once the 1,000 embedding requests are completed, the embedding GPU sits idle, while the generation model GPUs remain busy serving the remaining requests.

SameGPU deployment with FCFS achieves lower generation latency, because all 4 ORTHRUS instances can process generation requests. However, because SameGPU FCFS alternates between request types, embedding requests are forced to wait behind generation requests, producing a long tail in the embedding latency distribution. ORTHRUS deployment with FCFS improves upon SameGPU with FCFS, as it batches requests across types. As generation requests begin to finish, embedding requests are batched together and served. However, because FCFS does not distinguish between request types, embedding requests are still blocked behind a large number of generation requests, leading to a long tail in the embedding latency distribution.

ORTHRUS with IBS achieves low latency for both embedding and generation requests. The 99th percentile generation latency is reduced by 9% compared to SplitGPU (89 ms $\rightarrow$ 81 ms). For embedding, IBS lowers the 99th percentile latency by 16% compared to other schedulers (87 ms $\rightarrow$ 73 ms), while remaining within 16 ms of SplitGPU, which dedicates a GPU to embedding. These results show that IBS avoids embedding starvation while still reducing generation latency.

4.4 ORTHRUS ALLOWS HIGH GPU UTILIZATION WITH INSTANTANEOUS LOAD BALANCING

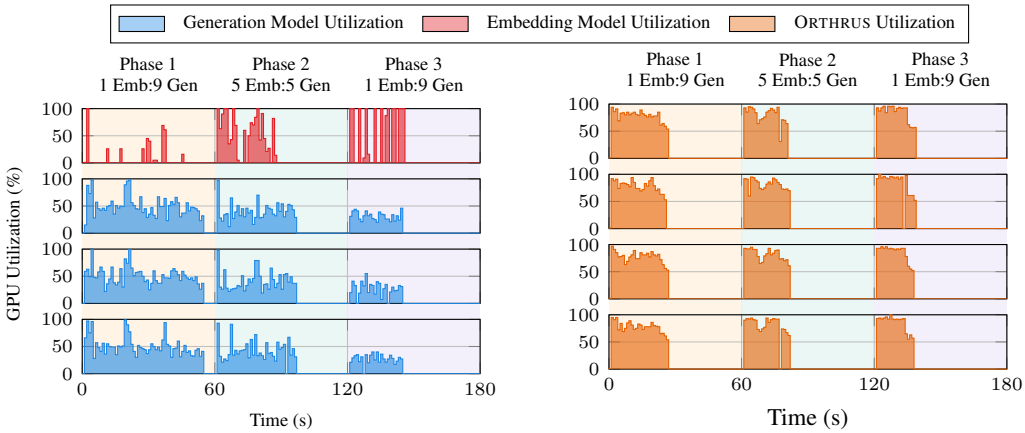

(a) Homogeneous batching with SplitGPU$_{1:3}$ (b) Heterogeneous batching with ORTHRUS

Figure 5: GPU utilization comparison between homogeneous batching (SplitGPU$_{1:3}$, Fig. 5a) and heterogeneous batching (ORTHRUS, Fig. 5b) under three phases of mixed workloads. In SplitGPU$_{1:3}$, the dedicated embedding GPU is severely underutilized in Phase 1, and generation GPUs in Phase 3, leading to lower average utilization (38%) and slower completion. In contrast, ORTHRUS keeps all GPUs uniformly busy across phases, sustaining much higher utilization (79%) and completing each phase 43% faster on average.

We evaluate the GPU utilization over different phases of request patterns to compare the load balancing capabilities of ORTHRUS, against a SplitGPU$_{1:3}$ deployment. The workload consists of three phases of 60 seconds each, with 1,000 requests per phase: Phase 1 has 10% embedding and 90% generation requests, Phase 2 has a 50/50 split, and Phase 3 has 90% embedding and 10% generation. Fig. 5 shows GPU utilization over time for both systems.

Overall, ORTHRUS completes each phase faster than SplitGPU, finishing requests an average 43% sooner. This improvement stems from higher GPU utilization: SplitGPU averages 38% during execution, whereas ORTHRUS reaches 79% (+40.6 pp). The gap is most pronounced in Phase 1, where the embedding GPU in SplitGPU is underutilized while ORTHRUS keeps all GPUs busy.

4.5 ORTHRUS SERVES BOTH REQUEST TYPES WITH MINIMAL OVERHEAD

We evaluate whether ORTHRUS can serve both embedding and generation requests on a single GPU without reducing throughput compared to dedicated deployments. We run embedding-only and generation-only workloads while varying concurrency from 1 to 256 clients. For embeddings (Fig. 6a), ORTHRUS achieves throughput close to a dedicated embedding model, with only a minor drop from LoRA overhead. For generation (Fig. 6b), ORTHRUS matches the dedicated generation

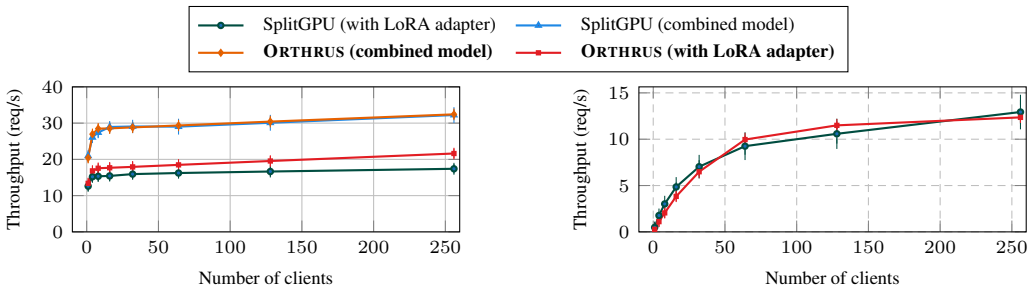

(a) Embedding throughput (1 GPU)

(b) Generation throughput (1 GPU)

Figure 6: Overhead analysis of ORTHRUS's heterogeneous batching. We plot throughput vs. number of clients on a single GPU for embedding-only (Fig. 6a) and generation-only (Fig. 6b) workloads. ORTHRUS achieves throughput comparable to dedicated vLLM SplitGPU deployments. Embedding throughput shows only a small drop due to LoRA overhead, while generation throughput matches SplitGPU across all concurrency levels.

deployment across all concurrency levels. Together, these results show that ORTHRUS preserves throughput for both request types while enabling them to share the same GPU.

4.6 ORTHRUS IS GENERALIZABLE TO OTHER MODELS

Table 1: Generalizability analysis by comparing throughput across different models and request mixes. We report embedding, generation, and the normalized throughput (Weighted Sum = Embed+ $1.7 \times$ Gen) for three ratios (9:1, 5:5, 1:9; embedding:generation). SplitGPU baseline runs separate models on a 1:3 GPU split. ORTHRUS co-locates both tasks on every GPU.

Model	Variant	9 Emb:1 Gen			5 Emb:5 Gen			1 Emb:9 Gen		
		Embed	Gen	Weighted Sum	Embed	Gen	Weighted Sum	Embed	Gen	Weighted Sum
Mistral 7B	$\text{SplitGPU}_{1:3}$	15.64	1.49	18.02	12.54	11.97	32.89	5.10	29.56	55.35
	ORTHRUS (e5-mistral LoRA)	58.80	7.00	**70.07**	25.32	26.24	**69.93**	4.20	39.10	**70.67**
Qwen2 7B	$\text{SplitGPU}_{1:3}$	13.23	1.72	16.15	10.72	10.08	27.86	2.81	27.76	50.00
	ORTHRUS (LoRA Rank 32)	40.90	4.40	**48.38**	26.80	25.93	**70.88**	6.20	48.23	**88.19**
LLaMA3.1 8B	$\text{SplitGPU}_{1:3}$	13.43	1.32	15.67	10.18	9.95	27.10	3.06	25.63	46.63
	ORTHRUS (LoRA Rank 64)	56.46	5.90	**66.49**	34.60	37.50	**98.35**	4.23	47.32	**84.674**

Finally, we evaluate the generalizability of ORTHRUS across different models and LoRA ranks. We run experiments with Qwen2 7B (Yang et al., 2024) and LLaMA3.1 8B (Grattafiori et al., 2024), in addition to Mistral 7B, using synthesized LoRA adapters for embedding models. We vary the ratio of embedding to generation requests and report throughput for each configuration. Table 1 summarizes the results.

Across all models and request ratios, ORTHRUS consistently outperforms $\text{SplitGPU}_{1:3}$. Even under extreme skews (e.g., 9:1 or 1:9), ORTHRUS sustains high throughput. For example, with Mistral 7B at a 9:1 ratio, ORTHRUS achieves up to $3.8\times$ higher throughput than the baseline. These results demonstrate that ORTHRUS generalizes across different models and LoRA ranks, providing robust performance improvements over SplitGPU deployments. This suggests that ORTHRUS can be broadly applied to mixed embedding-generation workloads in diverse LLM serving scenarios.

5 CONCLUSION

This work presents ORTHRUS, a serving system that unifies embedding and generation within a unified model runner through heterogeneous batching. Unlike existing systems, ORTHRUS integrates embedding into the same scheduling and execution path as generation. With its new mechanisms, ORTHRUS achieves higher throughput and lower latency under mixed workloads, enabling efficient serving for modern knowledge-intensive LLM applications.

Reproducibility Statement

We release anonymized source code and experiment scripts at `https://anonymous.4open.science/r/Orthrus-483B`. Our repository contains instructions for setting up the environment, launching experiments, and reproducing all figures and tables in the paper. The detailed evaluation setup is described in Section 4.1, and we provide configuration files for all baseline and ORTHRUS deployments. Together, these resources ensure that our results can be replicated and extended by the research community.

Ethics Statement

This work does not involve human subjects, proprietary datasets, or personally identifiable information. Our contributions focus on system design for efficiently serving existing open-weight LLMs. Potential risks are those inherent to large language models, such as misuse for generating harmful content, which are unchanged by our methods. Finally, we used an LLM only for grammar checking in writing this paper.

References

Amey Agrawal, Nitin Kedia, Ashish Panwar, Jayashree Mohan, Nipun Kwatra, Bhargav Gulavani, Alexey Tumanov, and Ramachandran Ramjee. Taming Throughput-Latency Tradeoff in LLM Inference with Sarathi-Serve. pp. 117–134, 2024. ISBN 978-1-939133-40-3. URL `https://www.usenix.org/conference/osdi24/presentation/agrawal`.

Akari Asai, Zeqiu Wu, Yizhong Wang, Avirup Sil, and Hannaneh Hajishirzi. Self-RAG: Learning to Retrieve, Generate, and Critique through Self-Reflection. October 2023. URL `https://openreview.net/forum?id=hSyW5go0v8`.

Parishad BehnamGhader, Vaibhav Adlakha, Marius Mosbach, Dzmitry Bahdanau, Nicolas Chapados, and Siva Reddy. LLM2Vec: Large Language Models Are Secretly Powerful Text Encoders, August 2024. URL `http://arxiv.org/abs/2404.05961`. arXiv:2404.05961 [cs].

Lequn Chen, Zihao Ye, Yongji Wu, Danyang Zhuo, Luis Ceze, and Arvind Krishnamurthy. Punica: Multi-Tenant LoRA Serving. *Proceedings of Machine Learning and Systems*, 6: 1–13, May 2024. URL `https://proceedings.mlsys.org/paper_files/paper/2024/hash/054de805fcceb78a201f5e9d53c85908-Abstract-Conference.html`.

Jiarui Fang, Yang Yu, Chengduo Zhao, and Jie Zhou. TurboTransformers: an efficient GPU serving system for transformer models. In *Proceedings of the 26th ACM SIGPLAN Symposium on Principles and Practice of Parallel Programming*, PPoPP '21, pp. 389–402, New York, NY, USA, 2021. Association for Computing Machinery. ISBN 978-1-4503-8294-6. doi: 10.1145/3437801.3441578. URL `https://dl.acm.org/doi/10.1145/3437801.3441578`.

Luyu Gao, Xueguang Ma, Jimmy Lin, and Jamie Callan. Precise Zero-Shot Dense Retrieval without Relevance Labels. In Anna Rogers, Jordan Boyd-Graber, and Naoaki Okazaki (eds.), *Proceedings of the 61st Annual Meeting of the Association for Computational Linguistics (Volume 1: Long Papers)*, pp. 1762–1777, Toronto, Canada, July 2023. Association for Computational Linguistics. doi: 10.18653/v1/2023.acl-long.99. URL `https://aclanthology.org/2023.acl-long.99/`.

Thomas Gauthier. Lord: Low-rank decomposition of finetuned large language models. `https://github.com/thomasgauthier/LoRD`, 2024. GitHub repository; commit fe03a8c (2024-05-02). Accessed 2025-09-19.

Aaron Grattafiori, Abhimanyu Dubey, Abhinav Jauhri, Abhinav Pandey, Abhishek Kadian, Ahmad Al-Dahle, Aiesha Letman, Akhil Mathur, Alan Schelten, Alex Vaughan, Amy Yang, Angela Fan, Anirudh Goyal, Anthony Hartshorn, Aobo Yang, Archi Mitra, Archie Sravankumar, Artem Korenev, Arthur Hinsvark, Arun Rao, Aston Zhang, Aurelien Rodriguez, Austen Gregerson, Ava Spataru, Baptiste Roziere, Bethany Biron, Binh Tang, Bobbie Chern, Charlotte Caucheteux, Chaya Nayak, Chloe Bi, Chris Marra, Chris McConnell, Christian Keller, Christophe Touret, Chunyang Wu, Corinne Wong, Cristian Canton Ferrer, Cyrus Nikolaidis, Damien Allonsius,

Daniel Song, Danielle Pintz, Danny Livshits, Danny Wyatt, David Esiobu, Dhruv Choudhary, Dhruv Mahajan, Diego Garcia-Olano, Diego Perino, Dieuwke Hupkes, Egor Lakomkin, Ehab AlBadawy, Elina Lobanova, Emily Dinan, Eric Michael Smith, Filip Radenovic, Francisco Guzmán, Frank Zhang, Gabriel Synnaeve, Gabrielle Lee, Georgia Lewis Anderson, Govind Thattai, Graeme Nail, Gregoire Mialon, Guan Pang, Guillem Cucurell, Hailey Nguyen, Hannah Korevaar, Hu Xu, Hugo Touvron, Iliyan Zarov, Imanol Arrieta Ibarra, Isabel Kloumann, Ishan Misra, Ivan Evtimov, Jack Zhang, Jade Copet, Jaewon Lee, Jan Geffert, Jana Vranes, Jason Park, Jay Mahadeokar, Jeet Shah, Jelmer van der Linde, Jennifer Billock, Jenny Hong, Jenya Lee, Jeremy Fu, Jianfeng Chi, Jianyu Huang, Jiawen Liu, Jie Wang, Jiecao Yu, Joanna Bitton, Joe Spisak, Jongsoo Park, Joseph Rocca, Joshua Johnstun, Joshua Saxe, Junteng Jia, Kalyan Vasuden Alwala, Karthik Prasad, Kartikeya Upasani, Kate Plawiak, Ke Li, Kenneth Heafield, Kevin Stone, Khalid El-Arini, Krithika Iyer, Kshitiz Malik, Kuenley Chiu, Kunal Bhalla, Kushal Lakhotia, Lauren Rantala-Yeary, Laurens van der Maaten, Lawrence Chen, Liang Tan, Liz Jenkins, Louis Martin, Lovish Madaan, Lubo Malo, Lukas Blecher, Lukas Landzaat, Luke de Oliveira, Madeline Muzzi, Mahesh Pasupuleti, Mannat Singh, Manohar Paluri, Marcin Kardas, Maria Tsimpoukelli, Mathew Oldham, Mathieu Rita, Maya Pavlova, Melanie Kambadur, Mike Lewis, Min Si, Mitesh Kumar Singh, Mona Hassan, Naman Goyal, Narjes Torabi, Nikolay Bashlykov, Nikolay Bogoychev, Niladri Chatterji, Ning Zhang, Olivier Duchenne, Onur Çelebi, Patrick Alrassy, Pengchuan Zhang, Pengwei Li, Petar Vasic, Peter Weng, Prajjwal Bhargava, Pratik Dubal, Praveen Krishnan, Punit Singh Koura, Puxin Xu, Qing He, Qingxiao Dong, Ragavan Srinivasan, Raj Ganapathy, Ramon Calderer, Ricardo Silveira Cabral, Robert Stojnic, Roberta Raileanu, Rohan Maheswari, Rohit Girdhar, Rohit Patel, Romain Sauvestre, Ronnie Polidoro, Roshan Sumbaly, Ross Taylor, Ruan Silva, Rui Hou, Rui Wang, Saghar Hosseini, Sahana Chennabasappa, Sanjay Singh, Sean Bell, Seohyun Sonia Kim, Sergey Edunov, Shaoliang Nie, Sharan Narang, Sharath Raparthy, Sheng Shen, Shengye Wan, Shruti Bhosale, Shun Zhang, Simon Vandenhende, Soumya Batra, Spencer Whitman, Sten Sootla, Stephane Collot, Suchin Gururangan, Sydney Borodinsky, Tamar Herman, Tara Fowler, Tarek Sheasha, Thomas Georgiou, Thomas Scialom, Tobias Speckbacher, Todor Mihaylov, Tong Xiao, Ujjwal Karn, Vedanuj Goswami, Vibhor Gupta, Vignesh Ramanathan, Viktor Kerkez, Vincent Gonguet, Virginie Do, Vish Vogeti, Vítor Albiero, Vladan Petrovic, Weiwei Chu, Wenhan Xiong, Wenyin Fu, Whitney Meers, Xavier Martinet, Xiaodong Wang, Xiaofang Wang, Xiaoqing Ellen Tan, Xide Xia, Xinfeng Xie, Xuchao Jia, Xuewei Wang, Yaelle Goldschlag, Yashesh Gaur, Yasmine Babaei, Yi Wen, Yiwen Song, Yuchen Zhang, Yue Li, Yuning Mao, Zacharie Delpierre Coudert, Zheng Yan, Zhengxing Chen, Zoe Papakipos, Aaditya Singh, Aayushi Srivastava, Abha Jain, Adam Kelsey, Adam Shajnfeld, Adithya Gangidi, Adolfo Victoria, Ahuva Goldstand, Ajay Menon, Ajay Sharma, Alex Boesenberg, Alexei Baevski, Allie Feinstein, Amanda Kallet, Amit Sangani, Amos Teo, Anam Yunus, Andrei Lupu, Andres Alvarado, Andrew Caples, Andrew Gu, Andrew Ho, Andrew Poulton, Andrew Ryan, Ankit Ramchandani, Annie Dong, Annie Franco, Anuj Goyal, Aparajita Saraf, Arkabandhu Chowdhury, Ashley Gabriel, Ashwin Bharambe, Assaf Eisenman, Azadeh Yazdan, Beau James, Ben Maurer, Benjamin Leonhardi, Bernie Huang, Beth Loyd, Beto De Paola, Bhargavi Paranjape, Bing Liu, Bo Wu, Boyu Ni, Braden Hancock, Bram Wasti, Brandon Spence, Brani Stojkovic, Brian Gamido, Britt Montalvo, Carl Parker, Carly Burton, Catalina Mejia, Ce Liu, Changhan Wang, Changkyu Kim, Chao Zhou, Chester Hu, Ching-Hsiang Chu, Chris Cai, Chris Tindal, Christoph Feichtenhofer, Cynthia Gao, Damon Civin, Dana Beaty, Daniel Kreymer, Daniel Li, David Adkins, David Xu, Davide Testuggine, Delia David, Devi Parikh, Diana Liskovich, Didem Foss, Dingkang Wang, Duc Le, Dustin Holland, Edward Dowling, Eissa Jamil, Elaine Montgomery, Eleonora Presani, Emily Hahn, Emily Wood, Eric-Tuan Le, Erik Brinkman, Esteban Arcaute, Evan Dunbar, Evan Smothers, Fei Sun, Felix Kreuk, Feng Tian, Filippos Kokkinos, Firat Ozgenel, Francesco Caggioni, Frank Kanayet, Frank Seide, Gabriela Medina Florez, Gabriella Schwarz, Gada Badeer, Georgia Swee, Gil Halpern, Grant Herman, Grigory Sizov, Guangyi, Zhang, Guna Lakshminarayanan, Hakan Inan, Hamid Shojanazeri, Han Zou, Hannah Wang, Hanwen Zha, Haroun Habeeb, Harrison Rudolph, Helen Suk, Henry Aspegren, Hunter Goldman, Hongyuan Zhan, Ibrahim Damlaj, Igor Molybog, Igor Tufanov, Ilias Leontiadis, Irina-Elena Veliche, Itai Gat, Jake Weissman, James Geboski, James Kohli, Janice Lam, Japhet Asher, Jean-Baptiste Gaya, Jeff Marcus, Jeff Tang, Jennifer Chan, Jenny Zhen, Jeremy Reizenstein, Jeremy Teboul, Jessica Zhong, Jian Jin, Jingyi Yang, Joe Cummings, Jon Carvill, Jon Shepard, Jonathan McPhie, Jonathan Torres, Josh Ginsburg, Junjie Wang, Kai Wu, Kam Hou U, Karan Saxena, Kartikay Khandelwal, Katayoun Zand, Kathy Matosich, Kaushik Veeraraghavan, Kelly Michelena, Keqian Li, Kiran Jagadeesh, Kun Huang, Kunal Chawla, Kyle Huang, Lailin Chen, Lakshya Garg, Lavender A, Leandro Silva, Lee Bell,

Lei Zhang, Liangpeng Guo, Licheng Yu, Liron Moshkovich, Luca Wehrstedt, Madian Khabsa, Manav Avalani, Manish Bhatt, Martynas Mankus, Matan Hasson, Matthew Lennie, Matthias Reso, Maxim Groshev, Maxim Naumov, Maya Lathi, Meghan Keneally, Miao Liu, Michael L. Seltzer, Michal Valko, Michelle Restrepo, Mihir Patel, Mik Vyatskov, Mikayel Samvelyan, Mike Clark, Mike Macey, Mike Wang, Miquel Jubert Hermoso, Mo Metanat, Mohammad Rastegari, Munish Bansal, Nandhini Santhanam, Natascha Parks, Natasha White, Navyata Bawa, Nayan Singhal, Nick Egebo, Nicolas Usunier, Nikhil Mehta, Nikolay Pavlovich Laptev, Ning Dong, Norman Cheng, Oleg Chernoguz, Olivia Hart, Omkar Salpekar, Ozlem Kalinli, Parkin Kent, Parth Parekh, Paul Saab, Pavan Balaji, Pedro Rittner, Philip Bontrager, Pierre Roux, Piotr Dollar, Polina Zvyagina, Prashant Ratanchandani, Pritish Yuvraj, Qian Liang, Rachad Alao, Rachel Rodriguez, Rafi Ayub, Raghotham Murthy, Raghu Nayani, Rahul Mitra, Rangaprabhu Parthasarathy, Raymond Li, Rebekkah Hogan, Robin Battey, Rocky Wang, Russ Howes, Ruty Rinott, Sachin Mehta, Sachin Siby, Sai Jayesh Bondu, Samyak Datta, Sara Chugh, Sara Hunt, Sargun Dhillon, Sasha Sidorov, Satadru Pan, Saurabh Mahajan, Saurabh Verma, Seiji Yamamoto, Sharadh Ramaswamy, Shaun Lindsay, Shaun Lindsay, Sheng Feng, Shenghao Lin, Shengxin Cindy Zha, Shishir Patil, Shiva Shankar, Shuqiang Zhang, Shuqiang Zhang, Sinong Wang, Sneha Agarwal, Soji Sajuyigbe, Soumith Chintala, Stephanie Max, Stephen Chen, Steve Kehoe, Steve Satterfield, Sudarshan Govindaprasad, Sumit Gupta, Summer Deng, Sungmin Cho, Sunny Virk, Suraj Subramanian, Sy Choudhury, Sydney Goldman, Tal Remez, Tamar Glaser, Tamara Best, Thilo Koehler, Thomas Robinson, Tianhe Li, Tianjun Zhang, Tim Matthews, Timothy Chou, Tzook Shaked, Varun Vontimitta, Victoria Ajayi, Victoria Montanez, Vijai Mohan, Vinay Satish Kumar, Vishal Mangla, Vlad Ionescu, Vlad Poenaru, Vlad Tiberiu Mihailescu, Vladimir Ivanov, Wei Li, Wenchen Wang, Wenwen Jiang, Wes Bouaziz, Will Constable, Xiaocheng Tang, Xiaojian Wu, Xiaolan Wang, Xilun Wu, Xinbo Gao, Yaniv Kleinman, Yanjun Chen, Ye Hu, Ye Jia, Ye Qi, Yenda Li, Yilin Zhang, Ying Zhang, Yossi Adi, Youngjin Nam, Yu, Wang, Yu Zhao, Yuchen Hao, Yundi Qian, Yunlu Li, Yuzi He, Zach Rait, Zachary DeVito, Zef Rosnbrick, Zhaoduo Wen, Zhenyu Yang, Zhiwei Zhao, and Zhiyu Ma. The Llama 3 Herd of Models, November 2024. URL http://arxiv.org/abs/2407.21783. arXiv:2407.21783 [cs].

Cunchen Hu, Heyang Huang, Liangliang Xu, Xusheng Chen, Jiang Xu, Shuang Chen, Hao Feng, Chenxi Wang, Sa Wang, Yungang Bao, Ninghui Sun, and Yizhou Shan. Inference without Interference: Disaggregate LLM Inference for Mixed Downstream Workloads, January 2024. URL http://arxiv.org/abs/2401.11181. arXiv:2401.11181 [cs].

Albert Q. Jiang, Alexandre Sablayrolles, Arthur Mensch, Chris Bamford, Devendra Singh Chaplot, Diego de las Casas, Florian Bressand, Gianna Lengyel, Guillaume Lample, Lucile Saulnier, Lélio Renard Lavaud, Marie-Anne Lachaux, Pierre Stock, Teven Le Scao, Thibaut Lavril, Thomas Wang, Timothée Lacroix, and William El Sayed. Mistral 7B, October 2023a. URL http://arxiv.org/abs/2310.06825. arXiv:2310.06825 [cs].

Zhengbao Jiang, Frank Xu, Luyu Gao, Zhiqing Sun, Qian Liu, Jane Dwivedi-Yu, Yiming Yang, Jamie Callan, and Graham Neubig. Active Retrieval Augmented Generation. In Houda Bouamor, Juan Pino, and Kalika Bali (eds.), *Proceedings of the 2023 Conference on Empirical Methods in Natural Language Processing*, pp. 7969–7992, Singapore, February 2023b. Association for Computational Linguistics. doi: 10.18653/v1/2023.emnlp-main.495. URL https://aclanthology.org/2023.emnlp-main.495/.

Woosuk Kwon, Zhuohan Li, Siyuan Zhuang, Ying Sheng, Lianmin Zheng, Cody Hao Yu, Joseph Gonzalez, Hao Zhang, and Ion Stoica. Efficient Memory Management for Large Language Model Serving with PagedAttention. In *Proceedings of the 29th Symposium on Operating Systems Principles*, pp. 611–626, Koblenz Germany, October 2023. ACM. ISBN 979-8-4007-0229-7. doi: 10.1145/3600006.3613165. URL https://dl.acm.org/doi/10.1145/3600006.3613165.

Patrick Lewis, Ethan Perez, Aleksandra Piktus, Fabio Petroni, Vladimir Karpukhin, Naman Goyal, Heinrich Küttler, Mike Lewis, Wen-tau Yih, Tim Rocktäschel, Sebastian Riedel, and Douwe Kiela. Retrieval-Augmented Generation for Knowledge-Intensive NLP Tasks. In *Advances in Neural Information Processing Systems*, volume 33, pp. 9459–9474. Curran Associates, Inc., 2020. URL https://proceedings.neurips.cc/paper/2020/hash/6b493230205f780e1bc26945df7481e5-Abstract.html.

Xiaoxi Li, Yujia Zhou, and Zhicheng Dou. UniGen: A Unified Generative Framework for Retrieval and Question Answering with Large Language Models. *Proceedings of the AAAI Conference on Artificial Intelligence*, 38(8):8688–8696, March 2024. ISSN 2374-3468. doi: 10.1609/aaai.v38i8.28714. URL https://ojs.aaai.org/index.php/AAAI/article/view/28714.

Zehan Li, Xin Zhang, Yanzhao Zhang, Dingkun Long, Pengjun Xie, and Meishan Zhang. Towards General Text Embeddings with Multi-stage Contrastive Learning, August 2023. URL http://arxiv.org/abs/2308.03281. arXiv:2308.03281 [cs].

Yuanjie Lyu, Zihan Niu, Zheyong Xie, Chao Zhang, Tong Xu, Yang Wang, and Enhong Chen. Retrieve-Plan-Generation: An Iterative Planning and Answering Framework for Knowledge-Intensive LLM Generation. In Yaser Al-Onaizan, Mohit Bansal, and Yun-Nung Chen (eds.), *Proceedings of the 2024 Conference on Empirical Methods in Natural Language Processing*, pp. 4683–4702, Miami, Florida, USA, January 2024. Association for Computational Linguistics. doi: 10.18653/v1/2024.emnlp-main.270. URL https://aclanthology.org/2024.emnlp-main.270/.

Xueguang Ma, Liang Wang, Nan Yang, Furu Wei, and Jimmy Lin. Fine-Tuning LLaMA for Multi-Stage Text Retrieval. In *Proceedings of the 47th International ACM SIGIR Conference on Research and Development in Information Retrieval*, SIGIR '24, pp. 2421–2425, New York, NY, USA, 2024. Association for Computing Machinery. ISBN 979-8-4007-0431-4. doi: 10.1145/3626772.3657951. URL https://dl.acm.org/doi/10.1145/3626772.3657951.

Rui Meng, Ye Liu, Shafiq Rayhan Joty, Caiming Xiong, Yingbo Zhou, and Semih Yavuz. SFR-Embedding-Mistral: Enhance Text Retrieval with Transfer Learning, October 2024. URL https://www.salesforce.com/blog/sfr-embedding/.

Niklas Muennighoff. SGPT: GPT Sentence Embeddings for Semantic Search, August 2022. URL http://arxiv.org/abs/2202.08904. arXiv:2202.08904 [cs].

Niklas Muennighoff, Hongjin Su, Liang Wang, Nan Yang, Furu Wei, Tao Yu, Amanpreet Singh, and Douwe Kiela. Generative Representational Instruction Tuning. October 2024. URL https://openreview.net/forum?id=BC4lIvfSzv.

Deepak Narayanan, Keshav Santhanam, Fiodar Kazhamiaka, Amar Phanishayee, and Matei Zaharia. Heterogeneity-Aware Cluster Scheduling Policies for Deep Learning Workloads. pp. 481–498, 2020. ISBN 978-1-939133-19-9. URL https://www.usenix.org/conference/osdi20/presentation/narayanan-deepak.

Pratyush Patel, Esha Choukse, Chaojie Zhang, Aashaka Shah, Íñigo Goiri, Saeed Maleki, and Ricardo Bianchini. Splitwise: Efficient Generative LLM Inference Using Phase Splitting. In *51st ACM/IEEE Annual International Symposium on Computer Architecture, ISCA 2024, Buenos Aires, Argentina, June 29 - July 3, 2024*, pp. 118–132. IEEE, 2024. doi: 10.1109/ISCA59077.2024.00019.

Zhihong Shao, Yeyun Gong, Yelong Shen, Minlie Huang, Nan Duan, and Weizhu Chen. Enhancing Retrieval-Augmented Large Language Models with Iterative Retrieval-Generation Synergy. In Houda Bouamor, Juan Pino, and Kalika Bali (eds.), *Findings of the Association for Computational Linguistics: EMNLP 2023*, pp. 9248–9274, Singapore, February 2023. Association for Computational Linguistics. doi: 10.18653/v1/2023.findings-emnlp.620. URL https://aclanthology.org/2023.findings-emnlp.620/.

Tao Shen, Guodong Long, Xiubo Geng, Chongyang Tao, Yibin Lei, Tianyi Zhou, Michael Blumenstein, and Daxin Jiang. Retrieval-Augmented Retrieval: Large Language Models are Strong Zero-Shot Retriever. In Lun-Wei Ku, Andre Martins, and Vivek Srikumar (eds.), *Findings of the Association for Computational Linguistics: ACL 2024*, pp. 15933–15946, Bangkok, Thailand, August 2024. Association for Computational Linguistics. doi: 10.18653/v1/2024.findings-acl.943. URL https://aclanthology.org/2024.findings-acl.943/.

Ying Sheng, Lianmin Zheng, Binhang Yuan, Zhuohan Li, Max Ryabinin, Beidi Chen, Percy Liang, Christopher Re, Ion Stoica, and Ce Zhang. FlexGen: High-Throughput Generative Inference of Large Language Models with a Single GPU. In *Proceedings of the 40th International Conference on Machine Learning*, pp. 31094–31116. PMLR, July 2023. URL https://proceedings.mlr.press/v202/sheng23a.html. ISSN: 2640-3498.

Ying Sheng, Shiyi Cao, Dacheng Li, Coleman Hooper, Nicholas Lee, Shuo Yang, Christopher Chou, Banghua Zhu, Lianmin Zheng, Kurt Keutzer, Joseph E. Gonzalez, and Ion Stoica. SLoRA: Scalable Serving of Thousands of LoRA Adapters. *Proceedings of Machine Learning and Systems*, 6: 296–311, May 2024a. URL https://proceedings.mlsys.org/paper_files/paper/2024/hash/906419cd502575b617cc489a1a696a67-Abstract-Conference.html.

Ying Sheng, Shiyi Cao, Dacheng Li, Banghua Zhu, Zhuohan Li, Danyang Zhuo, Joseph E. Gonzalez, and Ion Stoica. Fairness in Serving Large Language Models. pp. 965–988, 2024b. ISBN 978-1-939133-40-3. URL https://www.usenix.org/conference/osdi24/presentation/sheng.

Jacob Mitchell Springer, Suhas Kotha, Daniel Fried, Graham Neubig, and Aditi Raghunathan. Repetition Improves Language Model Embeddings. October 2024. URL https://openreview.net/forum?id=Ahlrf2HGJR.

Yubao Tang, Ruqing Zhang, Jiafeng Guo, Maarten de Rijke, Yixing Fan, and Xueqi Cheng. Boosting Retrieval-Augmented Generation with Generation-Augmented Retrieval: A Co-Training Approach. In *Proceedings of the 48th International ACM SIGIR Conference on Research and Development in Information Retrieval*, SIGIR '25, pp. 2441–2451, New York, NY, USA, 2025. Association for Computing Machinery. ISBN 979-8-4007-1592-1. doi: 10.1145/3726302.3729907. URL https://dl.acm.org/doi/10.1145/3726302.3729907.

Harsh Trivedi, Niranjan Balasubramanian, Tushar Khot, and Ashish Sabharwal. Interleaving Retrieval with Chain-of-Thought Reasoning for Knowledge-Intensive Multi-Step Questions. In Anna Rogers, Jordan Boyd-Graber, and Naoaki Okazaki (eds.), *Proceedings of the 61st Annual Meeting of the Association for Computational Linguistics (Volume 1: Long Papers)*, pp. 10014–10037, Toronto, Canada, July 2023. Association for Computational Linguistics. doi: 10.18653/v1/2023.acl-long.557. URL https://aclanthology.org/2023.acl-long.557/.

Bhoomit Vasani, Jack FitzGerald, Anjie Fang, and Sushmit Vaish. Phlora: data-free post-hoc low-rank adapter extraction from full-rank checkpoint. *arXiv preprint arXiv:2509.10971*, 2025.

vLLM. Long Text Embedding with Chunked Processing - vLLM. URL https://docs.vllm.ai/en/latest/examples/online_serving/openai_embedding_long_text.html.

Liang Wang, Nan Yang, and Furu Wei. Query2doc: Query Expansion with Large Language Models. In *Proceedings of the 2023 Conference on Empirical Methods in Natural Language Processing*, pp. 9414–9423, Singapore, 2023. Association for Computational Linguistics. doi: 10.18653/v1/2023.emnlp-main.585. URL https://aclanthology.org/2023.emnlp-main.585.

Liang Wang, Nan Yang, Xiaolong Huang, Linjun Yang, Rangan Majumder, and Furu Wei. Improving Text Embeddings with Large Language Models. In Lun-Wei Ku, Andre Martins, and Vivek Srikumar (eds.), *Proceedings of the 62nd Annual Meeting of the Association for Computational Linguistics (Volume 1: Long Papers)*, pp. 11897–11916, Bangkok, Thailand, August 2024. Association for Computational Linguistics. doi: 10.18653/v1/2024.acl-long.642. URL https://aclanthology.org/2024.acl-long.642/.

Xiaohui Wang, Ying Xiong, Yang Wei, Mingxuan Wang, and Lei Li. LightSeq: A High Performance Inference Library for Transformers. In Young-bum Kim, Yunyao Li, and Owen Rambow (eds.), *Proceedings of the 2021 Conference of the North American Chapter of the Association for Computational Linguistics: Human Language Technologies: Industry Papers*, pp. 113–120, Online, June 2021. Association for Computational Linguistics. doi: 10.18653/v1/2021.naacl-industry.15. URL https://aclanthology.org/2021.naacl-industry.15/.

Bingyang Wu, Yinmin Zhong, Zili Zhang, Shengyu Liu, Fangyue Liu, Yuanhang Sun, Gang Huang, Xuanzhe Liu, and Xin Jin. Fast Distributed Inference Serving for Large Language Models, September 2024. URL http://arxiv.org/abs/2305.05920. arXiv:2305.05920 [cs].

An Yang, Baosong Yang, Binyuan Hui, Bo Zheng, Bowen Yu, Chang Zhou, Chengpeng Li, Chengyuan Li, Dayiheng Liu, Fei Huang, Guanting Dong, Haoran Wei, Huan Lin, Jialong Tang, Jialin Wang, Jian Yang, Jianhong Tu, Jianwei Zhang, Jianxin Ma, Jianxin Yang, Jin Xu, Jingren Zhou, Jinze Bai, Jinzheng He, Junyang Lin, Kai Dang, Keming Lu, Keqin Chen, Kexin Yang, Mei Li, Mingfeng Xue, Na Ni, Pei Zhang, Peng Wang, Ru Peng, Rui Men, Ruize Gao, Runji

Lin, Shijie Wang, Shuai Bai, Sinan Tan, Tianhang Zhu, Tianhao Li, Tianyu Liu, Wenbin Ge, Xiaodong Deng, Xiaohuan Zhou, Xingzhang Ren, Xinyu Zhang, Xipin Wei, Xuancheng Ren, Xuejing Liu, Yang Fan, Yang Yao, Yichang Zhang, Yu Wan, Yunfei Chu, Yuqiong Liu, Zeyu Cui, Zhenru Zhang, Zhifang Guo, and Zhihao Fan. Qwen2 Technical Report, September 2024. URL http://arxiv.org/abs/2407.10671. arXiv:2407.10671 [cs].

Gyeong-In Yu, Joo Seong Jeong, Geon-Woo Kim, Soojeong Kim, and Byung-Gon Chun. Orca: A distributed serving system for {Transformer-Based} generative models. In *16th USENIX Symposium on Operating Systems Design and Implementation (OSDI 22)*, pp. 521–538, 2022.

Caojin Zhang, Qiang Zhang, Ke Li, Sai Vidyaranya Nuthalapati, Benyu Zhang, Jason Liu, Serena Li, Lizhu Zhang, and Xiangjun Fan. GEM: Empowering LLM for both Embedding Generation and Language Understanding, June 2025. URL http://arxiv.org/abs/2506.04344. arXiv:2506.04344 [cs].

Yinmin Zhong, Shengyu Liu, Junda Chen, Jianbo Hu, Yibo Zhu, Xuanzhe Liu, Xin Jin, and Hao Zhang. DistServe: Disaggregating Prefill and Decoding for Goodput-optimized Large Language Model Serving. pp. 193–210, 2024. ISBN 978-1-939133-40-3. URL https://www.usenix.org/conference/osdi24/presentation/zhong-yinmin.